Applied Physics Letters ARTICLE scitation.org/journal/apl

# A coordinate system invariant formulation for space-charge limited current in vacuum

Cite as: Appl. Phys. Lett. **115**, 054101 (2019); doi: 10.1063/1.5115261
Submitted: 16 June 2019 · Accepted: 3 July 2019 ·
Published Online: 30 July 2019

View Online Export Citation CrossMark

Adam M. Darr[1] and Allen L. Garner[1,2,a)]

## AFFILIATIONS

[1]School of Nuclear Engineering, Purdue University, West Lafayette, Indiana 47907, USA
[2]School of Electrical and Computer Engineering, Purdue University, West Lafayette, Indiana 47907, USA

[a)]algarner@purdue.edu

## ABSTRACT

While space-charge limited emission current density $J_{cr}$ is calculated exactly for one-dimensional (1D) planar geometry, 1D cylindrical and spherical geometries require approximations such as the Langmuir-Blodgett (LB) equations or nonphysical assumptions. Using variational calculus (VC), we derive a differential equation from first principles to calculate $J_{cr}$ for any geometry. This yields exact, closed-form analytical solutions for 1D coaxial cylindrical and concentric spherical geometries that approach LB for sufficiently close cathode ($R_c$) and anode ($R_a$) radii. VC agrees better with simulations in cylindrical geometry than LB at $R_c/R_a = 0.5$. The analytical VC solutions also demonstrate the asymptotic behavior for $J_{cr}$. For cylindrical geometry, $J_{cr} \propto 1/R_c^2$ as $R_c/R_a$ approaches zero or infinity. For spherical geometry, $J_{cr} \propto 1/R_c^2$ as $R_c/R_a \to 0$ and $J_{cr} \propto R_a^2/R_c^4$ as $R_c/R_a \to \infty$.



Space-charge limited emission (SCLE) theory in vacuum was derived by Child[1] for planar geometry and by Langmuir for planar and coaxial cylindrical geometries.[2] Initially attributed to residual gas effects,[2] the poor agreement between experiments and theory for cylindrical SCLE was later attributed to secondary emission.[3] Simulations also significantly disagree with theory for cylindrical SCLE.[4] The Child-Langmuir (CL) law calculates planar SCLE; the Langmuir-Blodgett (LB) equations model SCLE for cylinders and spheres.[1,2,5,6] Classical CL and LB were derived for one-dimensional (1D) geometry assuming zero injection velocity. Subsequent theories have extended these calculations to nonzero injection velocity,[7–10] multiple dimensions,[11–15] and multiple charged species.[16]

Characterizing geometric effects on SCLE is important for designing modern devices, particularly magnetrons and nanodevices.[17–21] Many studies have added precision to LB,[7,8,22] applied numerical methods,[23–28] derived transit time models,[29,30] or made analytical approximations assuming no space-charge.[31,32] In this letter, we derive an analytical solution of Poisson's equation using variational calculus (VC) to calculate SCLE. Although numerical VC techniques have been used for SCLE,[27,28] we derive exact, closed-form solutions for SCLE in 1D planar, cylindrical, and spherical coordinate systems by starting from a coordinate system invariant representation obtained from first principles.

To calculate the SCLE current-voltage relationship, we begin with continuity,

$$J = \rho v, \tag{1}$$

with $J$ being the current density, $\rho$ the electron charge density, and $v$ the electron velocity. Assuming zero injection velocity and vacuum, the energy balance is

$$mv^2/2 = e\phi, \tag{2}$$

with $m$ being the electron mass, $e$ the electron charge, and $\phi$ the electric potential. Poisson's equation is

$$\nabla^2\phi = \rho/\epsilon_0, \tag{3}$$

where $\epsilon_0$ is the permittivity of free space. Combining (1)–(3) yields

$$J = \epsilon_0\nabla^2\phi\sqrt{2e\phi/m}. \tag{4}$$

For an emission area $A$, the total current is $I = JA$. Rewriting (4) in terms of $I$ and averaging with respect to path length yield

$$\langle I(\phi(s))\rangle = \epsilon_0\sqrt{e/m}\left(\frac{1}{D}\right)\int \nabla^2\phi(s)\sqrt{2\phi(s)}A(s)ds, \tag{5}$$

with differential path length $ds$ from the cathode to the anode, cross-sectional area $A(s)$, electric potential $\phi(s)$, and total path length

$D \equiv \int ds$. For 1D diodes, $D$ is the gap distance; for more geometrically complex devices such as cyclotrons, $D$ could represent a periodic path length. Generally, one may alternatively average $I$ with respect to volume.

We calculate $\phi(s)$ for SCLE by minimizing energy $W = \int P dt$, with power $P = V_g\langle I\rangle$ and fixed diode bias voltage $V_g$. Since SCLE is steady-state with respect to time, minimizing $\langle I\rangle$ using VC gives the SCLE limit for $\phi(s)$ by solving the Euler-Lagrange (EL) equation of (5) using diode boundary conditions. Using $\phi(s)$ in (4) gives the SCLE current density $J_{cr}$. In general, the EL equation for $N$ general coordinates $k$ is[33]

$$\frac{\partial f}{\partial \phi} + \sum_{k=1}^{N} \frac{\partial^2}{\partial k^2}\left(\frac{\partial f}{\partial \phi_{kk}}\right) - \frac{\partial}{\partial k}\left(\frac{\partial f}{\partial \phi_k}\right) = 0, \tag{6}$$

with partial derivatives denoted by subscripts ($\phi_k \equiv \partial\phi/\partial k$) and $f$ is a function of $\phi$, $k$, and the partial derivatives of $\phi$. From (5), $f \equiv \nabla^2\phi(s)\sqrt{2\phi(s)}A(s)$; for Cartesian, cylindrical, and spherical coordinates, (6) gives

$$\nabla^2\phi = \frac{|\nabla\phi|^2}{4\phi}. \tag{7}$$

Equation (7) is general for every orthogonal coordinate system; for a demonstration, see the supplementary material. For boundary conditions, we set $\phi = 0$ at the cathode and $\phi = V_g$ at the anode. To find the SCLE limit for the planar diode, we solve (7) in Cartesian coordinates with $\phi(0) = 0$ and $\phi(D) = V_g$ and area $A(x)$ set to a constant. Solving (7) for the potential function in the planar case yields

$$\phi_p(x) = V_g(x/D)^{4/3}. \tag{8}$$

Notably, we obtain the same solution for $\phi'(0) = 0$, the other classic boundary condition for SCLE with zero injection velocity; this property also holds for cylindrical and spherical geometries. Combining (8) and (4) gives the planar SCLE emission current density $J_p$ from a completely analytical VC approach as

$$J_p = \frac{4V_g^{3/2}\epsilon_0\sqrt{2e/m}}{9D^2}, \tag{9}$$

which is identical to the traditional CL law,[1,2] validating that VC and the minimum current approach produce accurate SCLE results. This methodology is purely analytical, which is a significant advancement over previous efforts to apply VC to SCLE using numerical methods.[31,32]

We similarly solve (7) in cylindrical coordinates assuming axial and angular symmetry. The boundary conditions are $\phi(R_c) = 0$ and $\phi(R_a) = V_g$, where $R_c$ and $R_a$ are the cathode and anode radii, respectively. Noting $A(r) \propto r$ gives the cylindrical potential function as

$$\phi_c(r) = V_g\left[\frac{\ln(r/R_c)}{\ln(R_c/R_a)}\right]^{4/3}. \tag{10}$$

Combining (10) and (4) at $r = R_c$ yields

$$J_c = \frac{4V_g^{3/2}\epsilon_0\sqrt{2e/m}}{9R_c^2(\ln\bar{a})^2}, \tag{11}$$

for the VC cylindrical SCLE with $\bar{a} \equiv R_c/R_a$. For both cylinders and spheres, when the inner surface is the emitter, $\bar{a} \in (0, 1)$; for an external emitter, $\bar{a} \in (1, \infty)$. Equation (11) is an exact, closed-form solution from first principles that makes no assumptions on the form of $\phi_c(r)$. In comparison, LB used a series solution of (4) assuming $I \propto 1/(r\beta^2)$, yielding

$$J_{c,LB} = \frac{4V_g^{3/2}\epsilon_0\sqrt{2e/m}}{9R_cR_a\beta^2}, \tag{12}$$

with cylindrical geometric effects captured by $\beta = \beta(\bar{a})$, initially calculated for discrete increments of $\bar{a}$ using a power series expansion centered on $\bar{a} = 1$.[2,5,8,22] Further refinements to LB approximated $\beta$ as a function over several orders of magnitude of $\bar{a}$.[29] Comparing (11) and (12) implies $\beta^2 = \bar{a}(\ln\bar{a})^2$. The $(\ln\bar{a})^2$ factor raises serious concerns for the validity of the LB model for $\bar{a}$ far from unity. While other proposed solutions for cylindrical SCLE exist, they rely on nonphysical approximations such as assuming a non-SCLE $\phi(r)$[29,30] or setting $\phi_r = 0$ in (3) near the cathode.[30] Since the nature of SCLE is that the space-charge alters $\phi$ and $\phi_{rr} \neq 0$, $\phi_r = 0$ only at the cathode surface and nowhere else.

Figure 1(a) compares (11), (12), and a theoretical approximation assuming $\phi'(r) = 0$ near the cathode,[30] and a transit time model using the non-SCLE potential function[29] for a constant inner radius of 1 cm and $V_g = 1$ V. All theories converge as $\bar{a} \to 1$, which corresponds to small gap distance $D \equiv |R_a - R_c|$. In the small gap limit, $\ln(\bar{a}) \approx D/R_a$ or $\ln(\bar{a}) \approx D/R_c$ for $R_c > R_a$ and $R_a < R_c$, respectively; for both cases, (11) reduces to (9). Physically, CL is the limiting behavior near $\bar{a} = 1$ because the anode and cathode surfaces are nearly parallel. The theories begin to disagree as $\bar{a}$ diverges from unity. As $\bar{a} \to \infty$, all theories agree within an order of magnitude and have similar slopes; however, the theories diverge dramatically (over a few orders of magnitude), although still with similar slopes, as $\bar{a} \to 0$. Since Refs. 29 and 30 rely on assumptions violating SCLE, their close agreement with LB suggests that the traditional LB equations do not account for all relevant physics, especially for $\bar{a}$ far from unity, whereas the VC solution is based upon SCLE physics and the analytical approach is valid for all $\bar{a}$.

To demonstrate the accuracy of the VC solution, we compared (11) and (12) with simulation data from a particle-in-cell (PIC) simulation for a cylindrical geometry with $R_c = 0.005$ m and $R_a = 0.01$ m ($\bar{a} = 0.5$).[4] LB gives $\beta^2 = 0.2793$ for $\bar{a} = 0.5$.[6] Figure 2 shows that, even at $\bar{a}$ close to unity, VC agrees better with the simulation results than LB, while also giving closed form solutions. The benefit of VC as $\bar{a} \to 0$ or $\bar{a} \to \infty$ is likely much more pronounced.

The slow variation of $\ln(\bar{a})^2$ as $\bar{a} \to 0$ and $\bar{a} \to \infty$ reduces (11) to

$$J_c|_{\bar{a}\to 0} = J_c|_{\bar{a}\to\infty} \approx \frac{4V_g^{3/2}\epsilon_0\sqrt{2e/m}}{9R_c^2\gamma^2} \propto \frac{1}{R_c^2}, \tag{13}$$

for both limits, with $\gamma \approx \ln(\bar{a}) \approx$ constant. Figure 1(b) plots the same theories as Fig. 1(a) with $V_g = 1$ V but with constant $R_c = 1$ cm. The asymptotes in Fig. 1(b) are for $\ln(\bar{a}) \approx \ln(400) \approx 6 = \gamma$; this highlights the symmetry between external and internal cathode diodes. As $\bar{a}$ diverges further from unity (in either direction), (13) shows that $J_c$ and $I$ become nearly constant.

Noting $A(r) \propto r^2$ and assuming angular symmetry, we solve (7) for spherical geometry with boundary conditions $\phi(0) = 0$ and $\phi(R_a) = V_g$ (s) to obtain the spherical potential function,

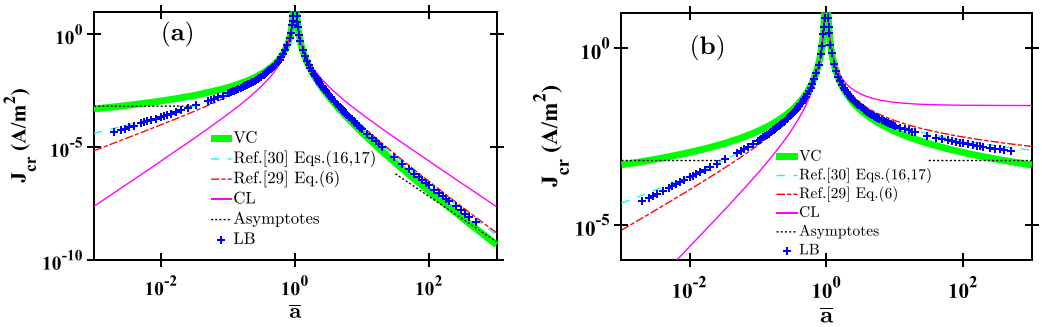


**FIG. 1.** Space-charge limited emission current density $J_{cr}$ for coaxial cylindrical diodes in vacuum as a function of $\bar{a} = R_c/R_a$ with a bias voltage of 1 V, cathode radius $R_c$, and anode radius $R_a$ for (a) a constant inner radius of 1 cm and for (b) constant $R_c = 1$ cm. The thicker solid line is the variational calculus (VC) solution (11), the dashed cyan line assumes the electric field is zero near the cathode Ref. 30, Eqs. (16) and (17), the dot-dashed red line assumes a potential function with no space-charge and solves numerically using the transit time solution from Ref. 29, the solid magenta line is the Child-Langmuir (CL) solution $J_p$ for planar geometry (9) with $D \equiv |R_c - R_a|$, the dotted black lines are the asymptotic limits of the VC solution (13) as $\bar{a} \to 0$ and $\bar{a} \to \infty$ for $\ln(\bar{a}) \approx 6$, and the blue plus marks are the Langmuir-Blodgett (LB) solution (12) using a power series approximation of Poisson's equation centered around $\bar{a} = 1$.

$$\phi_s(r) = V_g\left[\left(\frac{R_a}{R_a - R_c}\right)\left(1 - \frac{R_c}{r}\right)\right]^{4/3}. \tag{14}$$

Combining (14) with (4) at $r = R_c$ gives the VC spherical SCLE emission current density as

$$J_s = \frac{4V_g^{3/2}\epsilon_0\sqrt{2e/m}}{9\bar{a}^2D^2}, \tag{15}$$

where $D \equiv |R_a - R_c|$ is the gap distance. Analogous to the cylindrical case, (15) is an exact, closed-form solution from first principles that makes no assumptions on the form of $\phi_s(r)$. The original LB solution for spheres also used a series solution of (4), assuming $I \propto 1/(\alpha^2)$; this yields

$$J_{s,LB} = \frac{4V_g^{3/2}\epsilon_0\sqrt{2e/m}}{9R_c^2\alpha^2}, \tag{16}$$

with spherical geometric effects captured by $\alpha(\bar{a})$. A direct comparison between (15) and (16) suggests $\alpha^2 = (1 - \bar{a})^2$. Historically, $\alpha$ was calculated for discrete increments of $\bar{a}$[6] or approximated as an equation;[29] other refinements assume a non-SCLE potential function across the gap and use the cathode electric field or solve for $J$ numerically using a transit time model.[29] The problems posed by these simplifications are unchanged from their appearance in the cylindrical case.

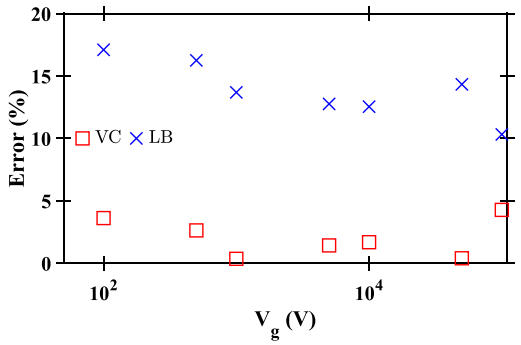


**FIG. 2.** Relative difference between a particle-in-simulation[4] of space-charge limited emission current density $J_{cr}$ for a coaxial cylindrical diode with a cathode radius of 0.005 cm and an anode radius of 0.01 cm ($\bar{a} = 0.5$) as a function of bias voltage $V_g$ with either the variational calculus (VC) solution (11) or the Langmuir-Blodgett solution (12). See the supplementary material for the data.

Figure 3(a) compares (15), (16), and Ref. 29 for a constant inner radius of 1 cm and $V_g = 1$ V; it shows that VC and the other theories agree well near $\bar{a} = 1$ where the solutions, including (15), reduce to (9); the solutions converge to the CL law because the anode and cathode become nearly parallel as $\bar{a} \to 1$. As $\bar{a} \to 0$, the theories diverge significantly in slope and magnitude; however, as $\bar{a} \to \infty$, the non-SCLE field and potential solutions match closely with LB, while VC, which has a fully SCLE potential function, diverges by over an order of magnitude.

Asymptotically, the limits of (15) as $\bar{a} \to 0$ and $\bar{a} \to \infty$ are

$$J_s|_{\bar{a}\to 0} \approx \frac{4V_g^{3/2}\epsilon_0\sqrt{2e/m}}{9R_c^2} \propto \frac{1}{R_c^2} \tag{17}$$

and

$$J_s|_{\bar{a}\to\infty} \approx \frac{4V_g^{3/2}\epsilon_0\sqrt{2e/m}}{9\bar{a}^2R_c^2} \propto \frac{1}{\bar{a}^2R_c^2} = \frac{R_a^2}{R_c^4}, \tag{18}$$

respectively.

Figure 3(b) highlights (17) and (18) by comparing SCLE $J$ with $R_c = 1$ cm for all $\bar{a}$. As $\bar{a} \to 0$, $J$ is completely independent of $R_a$, whereas as $\bar{a} \to \infty$, there is an additional dependence upon $\bar{a}$. Physically, $\bar{a} \to 0$ represents a central emitting cathode with a distant, relatively large anode and $\bar{a} \to \infty$ represents a large outer emitting cathode with a relatively small anode. To understand the differences between these limits, we compare the total emission current. Multiplying $J$ by the cathode area shows that $I \propto$ constant as $\bar{a} \to 0$ and $I \propto 1/\bar{a}^2$ as $\bar{a} \to \infty$. While the original LB derivation noted that the total current emission was independent of sphere size and depended only upon $\bar{a}$,[6] our results further demonstrate that the current is also completely independent of $\bar{a}$ when $\bar{a} \to 0$; Fig. 3 shows that (15) approaches (17) rapidly. We hypothesize that the cathode appears as a point emitter to the anode at these small aspect ratios;

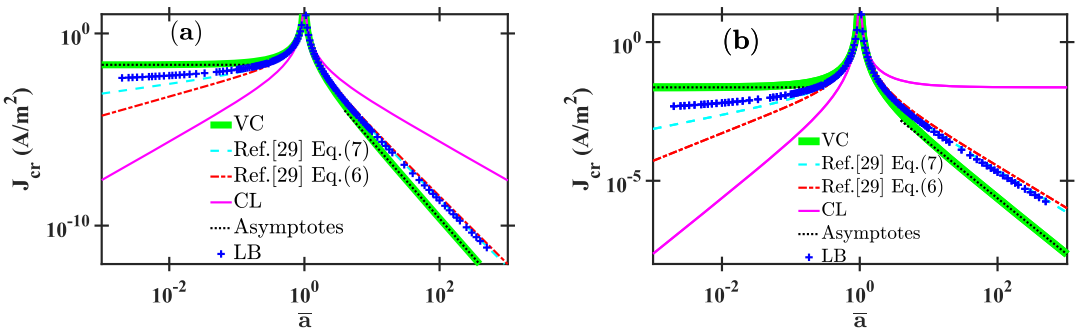


**FIG. 3.** Space-charge limited emission current density $J_{cr}$ for concentric spherical diodes in vacuum as a function of aspect ratio $\bar{a} = R_c/R_a$ with a bias voltage of 1 V, cathode radius $R_c$, and anode radius $R_a$ for (a) a constant inner radius of 1 cm and for (b) constant $R_c = 1$ cm. The thicker solid green line is the variational calculus (VC) solution (15), the dashed cyan line assumes the cathode electric field is the non-SCLE equation from Ref. 29, the dot-dashed red line assumes a potential function with no space-charge and solves numerically using the transit time Ref. 29, equation (6), the solid magenta line is the Child-Langmuir (CL) solution $J_p$ for planar geometry (9) with $D \equiv |R_c - R_a|$, the dotted black lines are the asymptotic limits of the VC solution (17) as $\bar{a} \to 0$ and (18) as $\bar{a} \to \infty$, and the blue plus marks are the Langmuir-Blodgett solution (12) which used a power series approximation of Poisson's equation centered around $\bar{a} = 1$.

therefore, increasing $R_a$ or decreasing $R_c$ no longer affects the total $I$. For $\bar{a} \to \infty$, the anode is now a point receiver, but we calculate emission current, and so $\bar{a}$ is still important. We hypothesize that when $\bar{a}$ increases, the relative surface areas of the cathode and anode increase as $\bar{a}^2$ and the emitted electrons crowd together as they travel to the anode. The increased electric field reduces the space-charge limit. This does not occur as $\bar{a} \to 0$ because the emitted electrons spread out during their transit from the cathode to the anode.

In summary, we used VC to bypass analytically unsolvable differential equations to derive exact analytical equations from first principles for SCLE emission for 1-D parallel plate (9), spherical (11), and cylindrical (15) geometries over all $\bar{a}$. The VC cylindrical solution matches simulation data much more accurately than LB even at $\bar{a}$ close to unity where LB is most applicable. To assess the validity of these VC solutions, we first showed that the VC approach yields the exact SCLE solution for parallel planar geometry, Eq. (9). For the curved geometries studied, the VC solution asymptotically approached the planar solution as $D$ became small ($\bar{a} \to 1$). As $\bar{a} \to 0$ and $\bar{a} \to \infty$, the VC solution has simpler asymptotic behavior, described in (13) for cylindrical geometries and (17) and (18) for spherical geometries. The full, asymptotic VC solutions have similar slopes at the extreme limits of $\bar{a}$ to past models except for the cylindrical geometry as $\bar{a} \to 0$. This asymptotic behavior and the exact nature of the VC solutions support our conclusion that VC yields the most physically accurate solution for SCLE in cylindrical and spherical geometries. The better agreement of VC theory with simulation compared to LB further supports the capabilities of this approach; future simulations and experiments at larger $\bar{a}$ may provide further validation.

VC may also be applied to multidimensional diodes,[12,30,34,35] including rough surfaces,[36] magnetically insulated transmission lines,[35,37] and recirculating magnetrons,[38] although these more complicated geometries will likely require numerical methods to solve the EL equation (7). One potential advantage of using VC over traditional numerical methods such as particle-in-cell (PIC) simulations is the stability offered in computing the potential and electric field in the diode. Moreover, since VC solves the steady-state condition rather than the time-dependent one, we anticipate that it will be more computationally efficient than PIC simulations, meaning that it will enable rapid screening of solutions that guide system design before performing more detailed PIC studies. Other theoretical applications for the VC approach include the quantum CL law,[39–42] relativistic CL,[43–45] optical field emission,[46,47] or transitions between SCLE and field emission either in vacuum[48] or with collisions.[49]

See the supplementary material for a detailed derivation and solutions of (7) and the data plotted in Fig. 2.

This material is based upon work supported by the Air Force Office of Scientific Research under Award No. FA9550-19-1-0101. A.M.D. gratefully acknowledges funding from a Purdue Doctoral Fellowship. We also gratefully acknowledge Sree Harsha Naropanth Ramamurthy, Peng Zhang, and John Luginsland for helpful discussions.

## REFERENCES

[1]C. D. Child, "Discharge from hot CaO," Phys. Rev. (Series I) **32**, 492–511 (1911).
[2]I. Langmuir, "The effect of space charge and residual gases on thermionic currents in high vacuum," Phys. Rev. **2**, 450–486 (1913).
[3]P. L. Walraven, "Test of Langmuir's three halves power law, deviations due to $\beta^2$-factor and secondary emission," Appl. Sci. Res., Sect. B **3**, 393–399 (1954).
[4]S. Mahalingam, C. Nieter, J. Loverich, D. Smithe, and P. Stoltz, "Space charge limited currents calculations in coaxial cylindrical didoes using particle-in-cell simulations," Open Plasma Phys. J. **2**, 63–69 (2009).
[5]I. Langmuir and K. Blodgett, "Currents limited by space charge between coaxial cylinders," Phys. Rev. **22**, 347–356 (1923).
[6]I. Langmuir and K. Blodgett, "Currents limited by space charge between concentric spheres," Phys. Rev. **24**, 49–59 (1924).
[7]L. Page and N. I. Adams, "Diode space charge for any initial velocity and current," Phys. Rev. **76**, 381–388 (1949).
[8]I. Itzkan, "Solutions of the equations of space charge flow for radial flow between concentric spherical electrodes," J. Appl. Phys. **31**, 652–655 (1960).
[9]J. H. Porter, W. Franzen, and R. S. Wenstrup, "A new analysis of space-charge-limited emission between concentric spheres and concentric cylinders," J. Appl. Phys. **43**, 344–354 (1972).
[10]L. H. Germer, "The distribution of initial velocities among thermionic electrons," Phys. Rev. **25**, 795–807 (1925).
[11]D. Lai, M. Qiu, Q. Xu, and Z. Huang, "Space-charge-limited currents for cathodes with electric field enhanced geometry," Phys. Plasmas **23**, 083104 (2016).

[12]Y. Y. Lau, "Simple theory for the two-dimensional Child-Langmuir law," Phys. Rev. Lett. **87**, 278301 (2001).
[13]J. W. Luginsland, Y. Y. Lau, and R. M. Gilgenbach, "Two-dimensional Child-Langmuir law," Phys. Rev. Lett. **77**, 4668 (1996).
[14]M. Zubair and L. K. Ang, "Fractional-dimensional Child-Langmuir law for a rough cathode," Phys. Plasmas **23**, 072118 (2016).
[15]W. S. Koh, L. K. Ang, and T. J. T. Kwan, "Three-dimensional Child-Langmuir law for uniform hot electron emission," Phys. Plasmas **12**, 053107 (2005).
[16]I. M. Rittersedorf, P. F. Ottinger, R. J. Allen, and J. W. Schumer, "Current density scaling expressions for a bipolar space-charge-limited cylindrical diode," IEEE Trans. Plasma Sci. **43**, 3626–3636 (2015).
[17]L. Page and N. I. Adams, "Space charge in cylindrical magnetron," Phys. Rev. **69**, 494–500 (1946).
[18]S. B. Swanekamp, R. J. Commisso, G. Cooperstein, P. F. Ottinger, and J. W. Schumer, "Particle-in-cell simulations of high-power cylindrical electron beam diodes," Phys. Plasmas **7**, 5214–5222 (2000).
[19]P. Y. Chen, T. C. Cheng, J. H. Tsai, and Y. L. Shao, "Space charge effects in field emission nanodevices," Nanotechnology **20**, 405202 (2009).
[20]L. Oksuz, "Analytical solution of space charge limited current for spherical and cylindrical objects," Appl. Phys. Lett. **88**, 181502 (2006).
[21]R. Kumar and D. Biswas, "Electromagnetic power loss in open coaxial diodes and the Langmuir-Blodgett law," Phys. Plasmas **17**, 104506 (2010).
[22]L. Page and N. I. Adams, "Space charge between coaxial cylinders," Phys. Rev. **68**, 126–129 (1945).
[23]R. Torres-Cordoba and E. Martinez-Garcia, "Analytical and exact solutions of the spherical and cylindrical diodes of Langmuir-Blodgett law," Phys. Plasmas **24**, 103113 (2017).
[24]C. B. Wheeler, "The approach to space charge limited current flow between coaxial cylinders," J. Phys. A **8**, 555–559 (1975).
[25]C. B. Wheeler, "The approach to space charge limited current flow between concentric spheres," J. Phys. A **8**, 1159–1163 (1975).
[26]C. B. Wheeler, "Space charge limited current flow between coaxial cylinders at potentials up to 15 MV," J. Phys. A **10**, 631–636 (1977).
[27]C. B. Wheeler, "Space charge limited current flow between concentric spheres at potentials up to 15 MV," J. Phys. A **10**, 1645–1649 (1977).
[28]L. Gold, "Transit time and space-charge for the cylindrical diode," J. Electron. Control **3**, 567–572 (1957).
[29]Y. B. Zhu, P. Zhang, A. Valfells, L. K. Ang, and Y. Y. Lau, "Novel scaling laws for the Langmuir-Blodgett solutions in cylindrical and spherical diodes," Phys. Rev. Lett. **110**, 265007 (2013).
[30]X. Chen, J. Dickens, L. L. Hatfield, E.-H. Choi, and M. Kristiansen, "Approximate analytical solutions for the space-charge-limited current in one-dimensional and two-dimensional cylindrical diodes," Phys. Plasmas **11**, 3278–3283 (2004).
[31]D. Anderson and M. Desaix, "Introduction to direct variational and moment methods and an application to the Child-Langmuir law," Eur. J. Phys. **36**, 065032 (2015).
[32]A. Rokhlenko, "Minimum current principle and variational method in theory of space charge limited flow," J. Appl. Phys. **118**, 153303 (2015).
[33]B. van Brunt, *The Calculus of Variations* (Universitext, New York, 2004).
[34]J. W. Luginsland, Y. Y. Lau, R. J. Umstattd, and J. J. Watrous, "Beyond the Child-Langmuir law: A review of recent results on multidimensional space-charge-limited flow," Phys. Plasmas **9**, 2371–2376 (2002).
[35]K. D. Bergeron, "Equivalent circuit approach to long magnetically insulated transmission lines," J. Appl. Phys. **48**, 3065–3069 (1977).
[36]Y. Y. Lau, "Effects of cathode surface roughness on the quality of electron beams," J. Appl. Phys. **61**, 36–44 (1987).
[37]R. W. Lemke, S. E. Calico, and M. C. Clark, "Investigation of a load-limited, magnetically insulated transmission line oscillator (MILO)," IEEE Trans. Plasma Sci. **25**, 364–374 (1997).
[38]S. M. Rossnagel and H. R. Kaufman, "Charge transport in magnetrons," J. Vac. Sci. Technol., A **5**, 2276 (1987).
[39]Y. Y. Lau, D. Chernin, D. G. Colombant, and P.-T. Ho, "Quantum extension of Child-Langmuir law," Phys. Rev. Lett. **66**, 1446–1449 (1991).
[40]L. K. Ang, T. J. T. Kwan, and Y. Y. Lau, "New scaling of Child-Langmuir law in the quantum regime," Phys. Rev. Lett. **91**, 208303 (2003).
[41]L. K. Ang, Y. Y. Lau, and T. J. T. Kwan, "Simple derivation of quantum scaling in Child-Langmuir law," IEEE Trans. Plasma Sci. **32**, 410–412 (2004).
[42]L. K. Ang and P. Zhang, "Ultrashort-pulse Child-Langmuir law in the quantum and relativistic regimes," Phys. Rev. Lett. **98**, 164802 (2007).
[43]E. W. V. Acton, "The space-charge limited flow of charged particles in planar, cylindrical and spherical diodes at relativistic velocities," J. Electron. Control **3**, 203–210 (1957).
[44]A. D. Greenwood, J. F. Hammond, P. Zhang, and Y. Y. Lau, "On relativistic space charge limited current in planar, cylindrical, and spherical diodes," Phys. Plasmas **23**, 072101 (2016).
[45]Y. L. Liu, S. H. Chen, W. S. Koh, and L. K. Ang, "Two-dimensional relativistic space charge limited current flow in the drift space," Phys. Plasmas **21**, 043101 (2014).
[46]M. Mitsunaga and R. G. Brewer, "Generalized perturbation theory of coherent optical emission," Phys. Rev. A **32**, 1605–1613 (1985).
[47]P. Hommelhoff, Y. Sortais, A. Aghajani-Talesh, and M. A. Kasevich, "Field emission tip as a nanometer source of free electron femtosecond pulses," Phys. Rev. Lett. **96**, 077401 (2006).
[48]Y. Y. Lau, Y. Liu, and R. K. Parker, "Electron emission: From the Fowler-Nordheim relation to the Child-Langmuir law," Phys. Plasmas **1**, 2082 (1994).
[49]A. M. Darr, A. M. Loveless, and A. L. Garner, "Unification of field emission and space charge limited emission with collisions," Appl. Phys. Lett. **114**, 014103 (2019).